Journal of Molecular Structure 1139 (2017) 160–165

Contents lists available at ScienceDirect

Journal of Molecular Structure

journal homepage: http://www.elsevier.com/locate/molstruc

Experimental and theoretical IR study of methyl thioglycolate, $CH_3OC(O)CH_2SH$, in different phases: Evidence of a dimer formation

Yanina B. Bava [a], Luciana M. Tamone [a], Luciana C. Juncal [a], Samantha Seng [b], Yeny A. Tobón [b], Sophie Sobanska [b], A. Lorena Picone [a], Rosana M. Romano [a, *]

[a] CEQUINOR (UNLP, CCT-CONICET La Plata), Departamento de Química, Facultad de Ciencias Exactas, Universidad Nacional de La Plata, Blvd. 120 N° 1465, La Plata, CP 1900, Argentina

[b] Laboratoire de Spectrochimie Infrarouge et Raman, UMR CNRS 8516, Université de Lille 1 Sciences et Technologies, Bât. C5, 59655, Villeneuve d'Ascq Cedex, France

ARTICLE INFO

Article history:
Received 26 November 2016
Received in revised form
15 February 2017
Accepted 7 March 2017
Available online 8 March 2017

Keywords:
Conformational analysis
Dimers
IR

ABSTRACT

The IR spectrum of methyl thioglycolate (MTG) was studied in three different phases, and interpreted with the aid of DFT calculations. The gas phase IR spectrum was explainable by the presence of the most stable conformer (*syn-gauche-(-)gauche*) only, while the IR spectrum of the liquid reveals strong intermolecular interactions, coincident with the formation of a dimeric form. The matrix-isolated spectra allow the identification of the second conformer (*syn-gauche-gauche*), in addition to the most stable form. The MTG dimer was also isolated by increasing the proportion of MTG in the matrix. The theoretical most stable structure of the dimer, which calculated IR spectrum agrees very well with the experimental one, is stabilized by a double interaction of the lone pair of the O atom of each of the C═O groups with the antibonding orbitals σ* (S–H).

1. Introduction

In a recent investigation, and as part of a general project dealing with photochemical studies of sulfur-containing compounds, we studied the gas-phase and matrix-isolated photolysis of MTG, followed by FTIR spectroscopy [1]. Although the Raman and infrared spectra of methyl thioglycolate in liquid phase has been reported previously, [2] as far as we know there are no vibrational studies of MTG in gas-phase or in matrix isolation conditions. The reported liquid-phase IR spectrum of MTG was interpreted by the presence of two conformers, denominated *cis* and *gauche*. However, the signals assigned to the second form were not observed in the IR spectrum of liquid MTG taken in the present work.

The microwave spectrum analysis of MTG was consistent with a structure with C_1 symmetry, with a double-minimum potential of a motion involving both HS-CC and SC-CO torsion, also predicted by *ab initio* calculations at the HF level [3,4,5]. In addition, the authors reported that a *Cs* structure with the hydrogen atom of the thiol group *trans* with respect to the C–C bond was 430 cm^{-1} (5.14 kJ mol^{-1}) less stable than the first form, while the *cis* conformer was found as a transition state [3].

For a correct interpretation of our photolysis experiments through the analysis of the FTIR spectra, a detailed analysis of the IR spectra of MTG in gas phase and matrix-isolated is required. Then, in this paper we present in the first place a complete theoretical conformational study, performed to help in the interpretation of the experimental spectroscopic findings. The calculation of the structure and IR spectrum of a dimeric form of MTG, $(MTG)_2$, is also included in this first part, since some features in the IR spectra are explainable in terms of the formation of the dimer. Secondly, the analysis of the IR spectra of gas, liquid and matrix-isolated MTG is presented.

2. Experimental and theoretical methods

A commercial sample of methyl thioglycolate (MTG, Aldrich 95%) was purified by repeated trap-to-trap distillation in vacuum conditions. Its purity was checked by means of gas phase FTIR spectrum. Ar (from AGA) was passed through a trap cooled to −100 °C to retain possible traces of impurities.

The IR spectra were taken on a Nexus Nicolet instrument equipped with either an MCTB or a DTGS detector (for the ranges

* Corresponding author.
E-mail address: romano@quimica.unlp.edu.ar (R.M. Romano).

http://dx.doi.org/10.1016/j.molstruc.2017.03.031
0022-2860/

4000–400 or 600-180 cm^{-1}, respectively). The IR spectrum of the neat liquid was measured between KBr windows at ambient temperatures, with a resolution of 4 cm^{-1}. A 10 cm-gas cell equipped with Si windows and a Young valve was employed to take the IR spectrum of the vapor, at ~3.5 mbar and ambient temperatures, with 1 and 0.5 cm^{-1} resolution.

The gaseous mixtures of MTG and Ar in different proportions were prepared by standard manometric methods. The matrices were formed by pulsed depositions [6,7] of the gas mixtures onto a cold CsI window (~10 K) of a Displex closed-cycle refrigerator (SHI-APD Cryogenics, model DE-202). In our experimental conditions, the IR spectra of the matrices were measured with a resolution of 0.125 and 0.5 cm^{-1}, with 256 and 64 scans, respectively.

All quantum chemical calculations were performed using the Gaussian 03 program package [8]. Geometry optimizations and transition state calculations were sought using standard gradient techniques by simultaneous relaxation of all geometrical parameters. The vibrational properties were calculated to characterize the structures as true minima, with no imaginary vibrational frequency, or as transition states.

The interaction energy (ΔE) in the MTG dimer structures were calculated and corrected for the basis set superposition error (BSSE) [9] using the counterpoise correction procedure proposed by Boys and Bernardi [10] and the zero-point energy differences. The bonding properties of MTG dimer were interpreted by natural bond orbital (NBO) analysis in terms of "donor-acceptor" interactions [12].

3. Results and discussion

3.1. Theoretical calculations

3.1.1. Conformational equilibrium of MTG

As mentioned in the introduction section, no complete conformational analysis for MTG has been reported. In this section, theoretical results obtained for the conformational properties of the title compound will be discussed. Various conformations of $CH_3OC(O)CH_2SH$ are feasible, depending mainly on the dihedral angles τ_1(C–O–C=O), τ_2(O=C–C–S) and τ_3(C–C–S–H) defined in Scheme 1.

All the combination between the three possible orientations *syn*, *anti* and *gauche* of these dihedral angles were explored (i.e. 27 conformers) by using the B3LYP/6-311 + G** approximation. Only six conformers were found as minima of the potential energy surface, depicted in Fig. S1 of the Supplementary Information. The dihedral angles τ_1, τ_2 and τ_3 obtained for these conformers are listed in Table S1 together with the calculated zero-point corrected energies and their estimated abundances at 298.15 K. The structure *syn-gauche*-(-)*gauche*, denominated conformer I, is predicted to be the most stable form at the level of theory employed, in coincidence with the microwave structure reported by Fantoni et al. [3]. The second stable form (*syn-gauche-gauche*, denominated conformer II) is found 1.02 kJ mol^{-1} higher in energy than conformer I. According to this approximation, the most stable conformer is predicted with an abundance of ~63% at ambient temperature, followed by conformer II with an abundance of ~34%. The predicted zero-point corrected energy difference between the two most stable conformers calculated using MP2/6-311 + G** model is 2.03 kJ mol^{-1} and the relative abundances at ambient temperatures are ~77% for the most stable form, ~23% for conformer II, and negligible (0.2%) for conformer III (see Table S2). Fig. 1 shows the optimized structures of the two most abundant conformers of MTG obtained using the B3LYP/6-311 + G** approximation. The geometrical parameters of conformers I, II and III calculated with both B3LYP and MP2 methods are presented as Supporting Information (Table S3). Table S4 lists the theoretical wavenumbers of the fundamental vibrational modes of conformers I and II of MTG calculated with the B3LYP/6-311 + G** approximation. The comparison of the IR simulated spectra of both conformers, depicted in Fig. S2, shows that there is only one vibrational mode sensitive to the conformation, assigned to the ν_{as} (C–C–O). This mode, predicted to be −23 cm^{-1} shifted in conformer II with respect to the same mode in the most stable form, can act as a sensor to detect possible conformational equilibrium, particularly in the matrix isolation spectra, characterized by narrow absorption bands.

A relaxed potential energy scan was performed varying τ_3(C–C–S–H) in steps of 10° using the B3LYP/6-311 + G** approximation, to localize the pathway for the conformational interconversion between conformers I and II. Two possible pathways were found, and the corresponding transition states, TS1 and TS2, characterized by one imaginary frequency, were optimized with the same theoretical model (see Fig. 2). The zero-point corrected energy barrier for the conformer I → conformer II conversion was calculated to be 9.28 kJ mol^{-1} through TS1 and 10.03 kJ mol^{-1} for the pathway involving TS2.

3.1.2. Dimer of MTG

The experimental findings observed for MTG isolated in Ar matrices will be discussed later in this paper. The FTIR spectra obtained when the proportion of MTG:Ar increases were interpreted in terms of the formation of a dimeric species. On the other hand, some important features found in the liquid phase FTIR spectrum of MTG, compared to the gas phase one, could also be interpreted in terms of associated species. To help in the interpretation of these experiments, to understand the origin of the interaction between the two subunits and also to predict the wavenumber shifts and the intensity changes in the FTIR spectra, a theoretical investigation of the MTG dimer was performed.

On the basis that molecules of MTG can interact by hydrogen bonds, attempts to optimize a dimeric structure were performed using B3LYP/6-31 + G* approximation. Fig. 3 shows the optimized molecular models for the two most stable dimers and Table S5 lists the calculated geometric parameters. The most stable dimer, $(MTG)_2$-I, is formed by the interaction of the two enantiomeric forms of conformer I of MTG. The second dimer, $(MTG)_2$-II, 0.91 kJ mol^{-1} higher in energy according to the B3LYP/6-31 + G* approximation, is composed by the same enantiomeric forms of conformer I. These structures, with a double hydrogen bond interaction, are similar to the reported dimers for related molecules like formic acid, [9–11] acetic acid, [12–15] and propionic acid [12]. The vibrational properties were also simulated to confirm that the structures correspond to energy minima with no imaginary

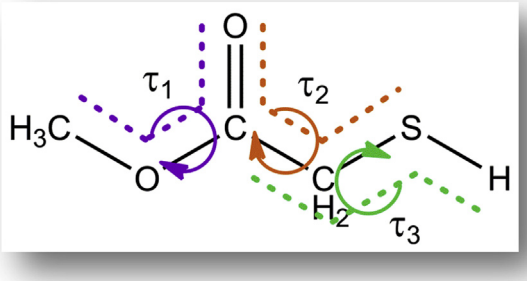

Scheme 1. Schematic representation of MTG showing the dihedral angles, τ_1 (C–O–C=O), τ_2 (O=C–C–S) and τ_3 (C–C–S–H), considered in the calculation of the different conformers.

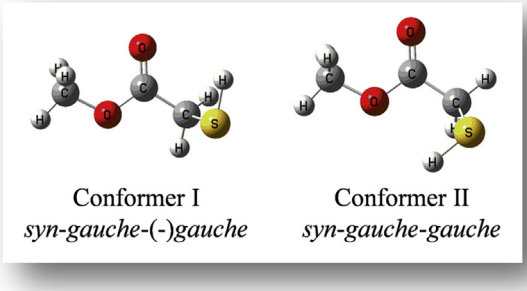

Fig. 1. Molecular models of the two most stable conformers of MTG calculated with the B3LYP/6-311 + G**.

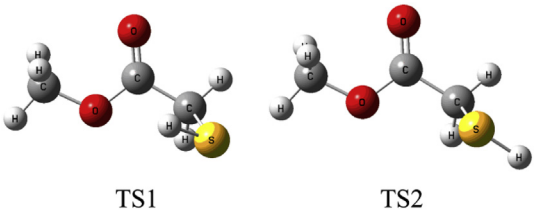

Fig. 2. Molecular models of the two transition states connecting the two most stable conformers of MTG calculated with the B3LYP/6-311 + G**.

frequencies, and to provide a basis for comparison with the experimental results. The most important predicted changes in the infrared spectrum induced by complexation of the free units are the shifts and intensification of ν (C═O) and ν (S–H) vibrational modes. For the most stable dimer, a red shift of 15 cm^{-1} is predicted for the ν (C═O) absorption with an intensification of ~3 times with respect to the monomers. For the ν (S–H) a splitting of the band and red shifts of ~33 and ~37 cm^{-1} are predicted, together with an important intensification of around 40 times of one of these bands with respect to the same absorption of the monomers.

Four other structures for the MTG dimer were also found as energy minima, with a calculated energy difference with respect to the most stable structure, according to the B3LYP/6-31 + G* approximation, of 2.68, $(MTG)_2$-III, 4.83, $(MTG)_2$-IV, 7.11, $(MTG)_2$-V, and 8.88, $(MTG)_2$-VI, kJ mol^{-1}, respectively. All these structures, which are depicted in Fig. S3 of the Supplementary Information, present also two hydrogen bond interactions, being the electron donor the oxygen atom either from the C═O or the methoxy groups, and the hydrogen either from the S–H or the methylene groups.

Taking into consideration not only the energy difference between of these structures with respect to the most stable dimer, but also the agreement between the experimental and calculated spectra, only the most stable dimer will be considered to explain and interpret the experimental findings.

The binding energy (ΔE) for the most stable dimeric structure was calculated using the correction proposed by Nagy et al. [16] which takes into account the counterpoise-corrected binding energy (ΔE^{CP}) due to the error of the basis set superposition (BSSE) and a term GEOM, that corresponds to the geometry changes experienced by MTG monomers on dimerization [17]. Values of −15.33 and −17.74 kJ mol^{-1} were calculated with the B3LYP/6-31 + G* theoretical model for the zero-point corrected binding energy (ΔE) and the counterpoise-corrected binding energy (ΔE^{CP}), respectively, the difference between these two quantities being attributable to the geometry changes mentioned before

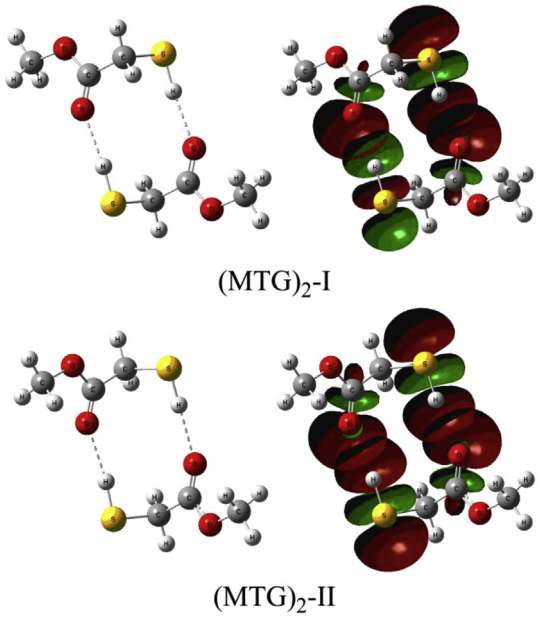

Fig. 3. Molecular models of the two most stable MTG dimers optimized with B3LYP/6-31 + G* approximation (left) and schematic representation of the orbital interactions using the Natural Bond Orbital (NBO) analysis (right).

(GEOM = 2.41 kJ mol^{-1}). The complete description of the binding energies calculations is described elsewhere [18].

NBO analysis was performed to investigate the bonding properties of the dimer in terms of "donor-acceptor" interactions [19]. According to this analysis, no net charge is transferred between the two subunits, each of them acting simultaneously either as a donor or an acceptor of charge. The largest contribution to the stabilization energy arises from the interaction of the lone pair of the O atom of the C═O groups with the antibonding orbitals σ* (S–H). The calculated value for the energy lowering due to each interaction, according to the B3LYP/6-31 + G* calculations, is 15.40 kJ mol^{-1}. Fig. 3 shows a schematic representation of the orbital interactions for the two most stable MTG dimers. The bonding character of the dimer can be also evaluated by the

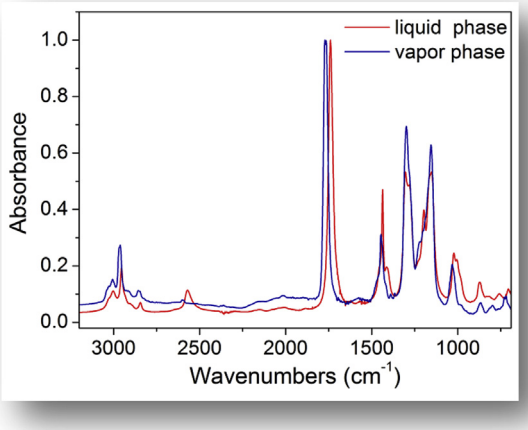

Fig. 4. FTIR spectrum of MTG in vapor-phase at ~3.5 mbar (blue trace) and in liquid-phase (red trace) in the 3200-690 cm^{-1} wavenumber region. (For interpretation of the references to colour in this figure legend, the reader is referred to the web version of this article.)

calculated van der Waals penetration distance d_p. [12]. This parameter is defined as the difference between the sum of the van der Waals radii of the interacting atoms and the equilibrium interatomic distance in the dimer. The calculated d_p distance for the MTG dimer is around 0.5 Å. This value indicates that the dimer can be interpreted in terms of the "donor-acceptor" model since it is accepted that this type of interaction prevails in complexes with $d_p \geq 0.1$ Å.

3.2. Experimental investigations

3.2.1. Gas and liquid phase IR spectra of MTG

A typical gas phase infrared spectrum of methyl thioglycolate is depicted in Fig. 4. To the best of our knowledge, the gas-phase spectrum of MTG was not previously reported. Table 1 lists the experimental wavenumbers observed in the gas-phase FTIR spectrum, together with the tentative assignment and the theoretical values calculated for the most stable conformer with the B3LYP/6-311 + G** approximation. The experimental gas phase IR spectrum can be fully interpreted by the presence of the most stable conformer only. This fact can be easily explained taken into consideration the expected similarity of the IR spectrum of the second conformer with respect to the most stable one, and the width of the IR absorption due to vibro-rotational transitions. The band shape analyses of some of the absorptions in the gas phase spectrum have been performed (Fig. S4). The P-R separations were predicted using the criteria explained by Seth-Paul [20] and compared with the experimental values (Table 1). As can be observed in the table, the predicted Δ(P-R) values are in good agreement with the experimental ones. The parameters used for these calculations were presented as Supplementary Information in Table S6.

Table 1
Vibrational wavenumbers (in cm^{-1}) of the IR spectra of methyl thioglycolate in gas-phase and isolated in solid Ar, together with the values calculated with the B3LYP/6-311 + G** theoretical approximation.

Experimental					B3LYP/6-311 + G** ν (cm^{-1})[a, b]	Tentative assignment[c]
Gas				Ar-matrix		
ν (cm^{-1})[a]	Band-shape	$\Delta\nu\ (P-R)_{exp}$	$\Delta\nu\ (P-R)_{theo}$	ν (cm^{-1})[a]		
3039 3030 3026 (5)	AC	13	13	3039.2 (2)	3066 (5)	ν_{as} (CH_3)
3012 3006 2998 (11)	AC	14	14	3011.6 (5)	3033 (6)	ν_{as} (CH_3)
2970 2965 2959 (25)	AB	11	10	2963.5 (11)	2998 (2)	ν_s (CH_2)
2913.5 (11)				2933.4 (3)	2962 (11)	ν_s (CH_3)
2602 2597 2592 (<1)	AB	10	10	2590.1 (<1)	2591 (0.2)	ν (S–H)
1773 1770 1764 (100)	B	9	9	1756.5 (100)	1734 (100)	ν (C=O)
1463 (13)				1461.5 (5)	1451 (4)	δ (CH_3)
1446 (10)				1449.6 1447.9 (7)	1439 (4)	δ (CH_3)
1437 (4)				14416 1439.7 (14)	1428 (10)	δ (CH_3)
1420 (9)				1416.5 1414.4 (6)	1418 (1)	δ (CH_2)
1300 (66)				1306.1 (73)	1274 (75)	ν_{as} (C–C–O)
				1296.9 (10)	1251	ν_{as} $(C-C-O)_{II}$
1281 (33)				1285.5 (10)	1219(39)	δ (CH_2)
1204 (45)				1197.8 1194.8 (36)	1171 (2)	δ (CH_3)
1169 (20)				1177.6 1174.9 (7)	1136 (5)	δ (CH_3)
1156 (62)				1171.5 1167.2 1158.3 1152.6 1146.4 (61)	1133 (49)	δ (CH_2)
1040 1033 1024 (19)	AC	16	16	1037.9 1033.7 1025.2 1011.7 1008.1 1748.1 (10)	1010 (15)	ν (O–CH_3)
867 (4)				880.3 (7)	846 (4)	ν_s (C–C–O)
729 (2)				767.6 (1)	805 (2)	δ (C–S–H)
720 (2)				713.8 (1)	733 (2)	δ_{oop} C=O
				660.8 (3)	684 (3)	ν (C–S)
570 (<1)				569.7 (1)	575 (3)	δ (C–C=O)

[a] Normalized intensities of conformer I in parentheses.
[b] Wavenumbers scaled by a 0.97 factor [21].
[c] ν_{as}, antisymmetric stretching; ν_s, symmetric stretching; δ, deformation; δ_{oop}, out-of-plane deformation.

The liquid phase infrared spectrum was also measured and compared with the one previously reported,[5] in which two absorption bands were observed in the carbonyl energy region, at 1740 and 1715 cm^{-1}, and assigned to the two most stable conformers. However, in the present study, only the band at 1740 cm^{-1} was observed, concluding that the feature at 1715 cm^{-1} could be due to the presence of an impurity in the liquid sample employed for the reported study [5]. On the other hand, the carbonyl absorption for the second stable structure (conformer II) is expected to appear at higher wavenumbers with respect to the one of conformer I, according to the B3LYP/6-311 + G** approximation. Fig. 4 also shows the infrared spectra of MTG in liquid phase recorded at ambient temperatures. It is important to note that a red shift of 27 cm^{-1} of the ν (S–H) vibrational mode, together with an important intensification, is observed in the liquid phase spectrum with respect to the same band in the gas phase spectrum. Moreover, the ν (C═O) mode in the liquid phase spectrum appears at 1740 cm^{-1}, with a ~30 cm^{-1} red shift compared to the corresponding one in the gas phase IR spectrum. The liquid phase IR spectrum of MTG, presented in Table 2, resembles the calculated IR spectrum for the dimeric specie, giving evidence of an important association of MTG molecules in the liquid phase, as previously reported for related molecules [22].

3.2.2. Matrix-isolated spectra of MTG

To the best of our knowledge, matrix isolation studies of MTG have not been reported so far. Gas mixtures of MTG with Ar in the proportions ca. 1:1000, 1:750 and 1:200 were prepared by standard manometric methods and deposited on a cooled CsI window, as described in the experimental section.

The IR absorptions observed in the IR spectrum of MTG isolated in solid Ar in a 1:1000 proportion (Fig. 5) are listed in Table 1. As expected from the analysis of the theoretical IR spectra presented above in this paper, only one absorption of conformer II, close to 1297 cm^{-1} and assigned to ν_{as} (C–C–O), is detected in the matrix-isolated spectrum.

Table 2
Vibrational wavenumbers (in cm^{-1}) of the IR absorptions assigned to methyl thioglycolate dimer, $(MTG)_2$, in liquid phase and isolated in solid Ar, together with the values calculated with the B3LYP/6-31 + G* theoretical approximation.

Liquid phase	Ar-matrix	B3LYP/6-31 + G*[a]		Tentative assignment[b]
		$(MTG)_2$-I	$(MTG)_2$-II	
2954	2959	3017 (<1)	3018 (1)	ν_s (CH_2)
		3017 (1)	3014 (1)	
2570	2566	2569 (27)	2588 (11)	ν (S–H) o.-p.
		2565 (<1)	2573 (12)	ν (S–H) i.-p.
1740	1747	1726 (100)	1727 (100)	ν (C═O) o.-p.
		1720 (<1)	1722 (7)	ν (C═O) i.-p.
1437	–	1468 (3)	1444 (4)	δ (CH_3); δ (CH_2) i.-p.
		1461 (2)	1434 (3)	
1414	–	1444 (6)		δ (CH_3); δ (CH_2) i.-p.
1281	1286	1291 (<1)	1290 (21)	ν_{as} (C–C–O) i.-p.
		1289 (67)	1287 (51)	ν_{as} (C–C–O) o.-p.
1192	1198	1156 (<1)	1156 (13)	δ (CH_2) i.p.
		1154 (34)	1153 (24)	δ (CH_2) o.-p.
	1033	1032 (11)	1031 (4)	δ (C–C–O) i.p.
		1032 (<1)	1029 (8)	δ (C–C–O) o.-p.
1004	1012	986 (<1)	987 (1)	δ (C–S–H); ν (C–C–O)
986	992	985 (2)	859 (1)	ν_s (C–C–O); δ (C–S–H)
706	709	685 (2)	684 (1)	ν (C–S)
585	598	577 (2)	576 (1)	δ (C–C═O); ν_s (C–C–S)
564	564	577 (<1)	575 (1)	δ (C–C═O); ν_s (C–C–S)
419	419	353 (8)	403 (1)	τ (C–C–S–H)

[a] Wavenumbers scaled by a 0.97 factor [19].
[b] ν_{as}, antisymmetric stretching; ν_s, symmetric stretching; δ, deformation; τ, torsion; i.-p. in phase; o.-p. out of phase.

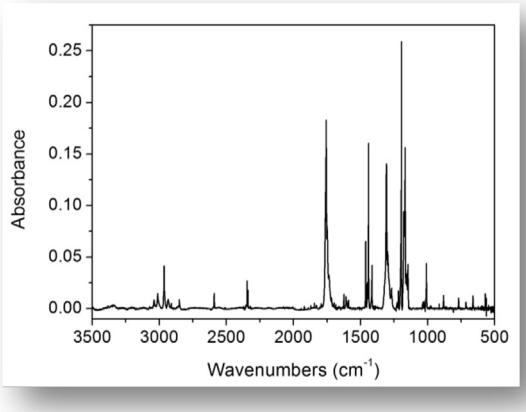

Fig. 5. FTIR spectrum of MTG isolated in solid Ar in the proportion 1:1000.

As the MTG proportion increases, the IR spectra of the matrices reveal several new absorptions that can be interpreted in terms of the existence of a dimeric structure of MTG. As mentioned earlier in the theoretical calculations section, the shifts and intensification of the ν (C═O) and ν (S–H) vibration modes are expected to be the most important features of the infrared spectrum of the dimer. Fig. 6 shows these two spectral regions when the proportion of MTG in the matrices increases. The absorption at 1747 cm^{-1} and the broad band centered at 2566 cm^{-1} were assigned to the ν (C═O) and ν (S–H) of a dimer, respectively. There is a good agreement between the calculated and experimental wavenumber shifts of these two vibrational modes induced by dimerization of the free subunits. In the case of ν (C═O) vibrational mode, the predicted shift of −15 cm^{-1} (B3LYP/6-31 + G*) agrees with the −10 cm^{-1} experimental shift. For the ν (S–H) vibrational mode a broad band approximately −24 cm^{-1} shifted matches the theoretical predictions.

Although the ν (C═O) and ν (S–H) absorptions are the most visible signals in the IR spectra that account for a dimer formation, several new bands, compiled in Table 2, are observed to increase with the MTG proportion in the matrices, and therefore assigned to a dimer. A very well agreement between these IR bands, the ones detected in the IR spectrum of the liquid, and the wavenumbers calculated for the most stable structures of MTG dimer reinforces this assignment.

4. Conclusions

The IR spectra of MTG in gas and liquid phases and also isolated in solid Ar were analysed and interpreted in terms of the molecular structure, aided by DFT calculations. The gas phase IR spectrum can be fully interpreted by the presence of the most stable conformer only, with *syn-gauche-(-)gauche* structure, corroborated by the band-shape analysis. On the other hand, the position and relative intensities of the absorptions in the liquid IR spectrum reveals strong intermolecular interactions, presumable through the formation of a dimeric form of MTG. The sharpening of the absorption bands in the matrix-isolated spectra with respect to the spectra in other phases allows the identification of the second conformer (*syn-gauche-gauche*), by the only absorption predicted with a sufficient wavenumber shift to be detected. The MTG dimer was also isolated by increasing the proportion of MTG in the matrix, and its IR spectrum was interpreted by comparison with the simulated IR

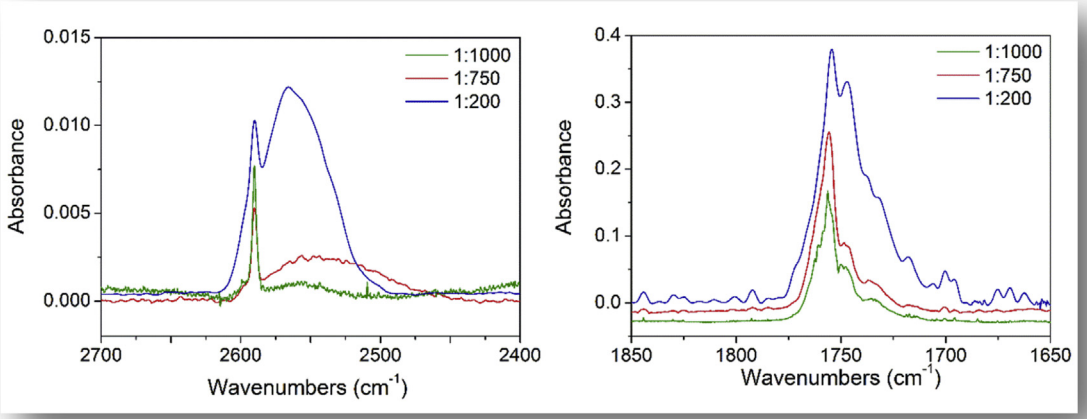

Fig. 6. FTIR spectra in the ν (S–H) (left) and ν (C=O) (right) spectral regions of MTG isolated in Ar in different MTG:Ar proportions: 1:1000 (green trace), 1:750 (red trace) and 1:200 (blue trace). (For interpretation of the references to colour in this figure legend, the reader is referred to the web version of this article.)

spectrum for the calculated most stable structures of the MTG dimer.

Acknowledgements

This work was supported by funds from the International cooperation program ECOS-MinCyT (A13E05), Agencia Nacional Científica y Tecnológica ANPCyT (PICT11-0647 and PICT14-3266), Facultad de Ciencias Exactas of the Universidad Nacional de La Plata (UNLP-11/X684), Consejo Nacional de Investigaciones Científicas y Técnicas CONICET (PIP-0352)) and the LABEXCaPPA PIA Program (contract ANR-11-LABX-0005-01).

Appendix A. Supplementary data

Supplementary data related to this article can be found at http://dx.doi.org/10.1016/j.molstruc.2017.03.031.

References

[1] Bava, Y. B; Tamone, L. M.; Juncal, L. C.; Seng, S.; Tobón, Y. A.; Sobanska S; Picone, A. L.; Romano, R. M. Gas-phase and matrix-isolation photochemistry of methyl thioglycolate, CH3OC(O)CH2SH: influence of the presence of molecular oxygen in the photochemical mechanisms. Submitted to J. Photochem. Photobiol. A. Chem.

[2] R. Das, S. Chattopadhyay, Vibrational spectra and rotational isomersm of some aliphatic molecules, Indian J. Pure Appl. Phys. 16 (1978) 482–485.

[3] A.C. Fantoni, W. Caminati, A double minimum motion and –S–H···O=C hydrogen bond in methylthioglycolate, J. Mol. Spectrosc. 143 (1990) 389–391.

[4] A.C. Fantoni, W. Caminati, P.G. Favero, The SH torsion double minimum potential in methylthioglycolate as studied by millimeterwave free jet absorption spectroscopy and ab initio investigations, J. Mol. Spectrosc. 176 (1996) 364–368.

[5] G. Maccaferri, W. Caminati, P.G. Favero, A.C. Fantoni, Millimeter-wave free jet absorption spectrum of SD methylthioglycolate: description of the SH torsion double minimum potential, J. Mol. Spectrosc. 186 (1997) 171–176.

[6] M.J. Almond, A.J. Downs, Spectroscopy of matrix isolated species, Adv. Specrosc. 17 (1989) 1–511. Dunkin, I. R. Matrix-Isolation Techniques: A Practical Approach, Oxford University Press, New York, 1998.

[7] R.N. Perutz, J.J. Turner, Pulsed matrix Isolation a comparative study, J. Chem. Soc. Faraday Trans. 2 (1973) 452–461, 69.

[8] M.J. Frisch, G.W. Trucks, H.B. Schlegel, G.E. Scuseria, M.A. Robb, J.R. Cheeseman, J.A. Montgomery Jr., T. Vreven, K.N. Kudin, J.C. Burant, J.M. Millam, S.S. Iyengar, J. Tomasi, V. Barone, B. Mennucci, M. Cossi, G. Scalmani, N. Rega, G.A. Petersson, H. Nakatsuji, M. Hada, M. Ehara, K. Toyota, R. Fukuda, J. Hasegawa, M. Ishida, T. Nakajima, Y. Honda, O. Kitao, H. Nakai, M. Klene, X. Li, J.E. Knox, H.P. Hratchian, J.B. Cross, V. Bakken, C. Adamo, J. Jaramillo, R. Gomperts, R.E. Strat-mann, O. Yazyev, A.J. Austin, R. Cammi, C. Pomelli, J.W. Ochterski, P.Y. Ayala, K. Morokuma, G.A. Voth, P. Salvador, J.J. Dannenberg, V.G. Zakrzewski, S. Dapprich, A.D. Daniels, M.C. Strain, O. Farkas, D.K. Malick, A.D. Rabuck, K. Raghavachari, J.B. Foresman, J.V. Ortiz, Q. Cui, A.G. Baboul, S. Clifford, J. Cioslowski, B.B. Ste-fanov, G. Liu, A. Liashenko, P. Piskorz, I. Komaromi, R.L. Martin, D.J. Fox, T. Keith, M.A. Al-Laham, C.Y. Peng, A. Nanayakkara, M. Challacombe, P.M.W. Gill, B. John-son, W. Chen, M.W. Wong, C. Gonzalez, J.A. Pople, Gaussian 03 Revision C.02, Gaussian Inc., Wallingford, CT, 2004.

[9] M. Halupka, W. Sander, A simple method for the matrix isolation of monomeric and dimeric carboxylic acids, Spectrochim. Acta Part A Mol. Biomol. Spectrosc. 54 (1998) 495–500.

[10] M. Gantenberg, M. Halupka, W. Sander, Dimerization of formic acid- an example of a "noncovalent" reaction mechanism, Chem. A Eur. J. 6 (2000) 1865–1869.

[11] K. Marushkevich, L. Khriachtchev, M. Räsänen, M. Melavuori, J. Lundell, Dimers of the higher-energy conformer of formic acid: experimental observation, J. Phys. Chem. A 116 (2012) 2101–2108.

[12] J. Chocholoušová, J. Vacek, P. Hobza, Acetic acid dimer in the gas phase, nonpolar solvent, microhydratedenvironment, and dilute and concentrated acetic acid: ab initio quantum chemical and molecular dynamics simulations, J. Phys. Chem. A 107 (2003) 3086–3092.

[13] W. Sander, M. Gantenberg, Aggregation of acetic and propionic acid in argon matrices—a matrix isolation and computational study, Spectrochim. Acta Part A Mol. Biomol. Spectrosc. 62 (2005) 902–909.

[14] A. Olbert-Majkut, J. Ahokas, J. Lundell, M. Pettersson, Raman spectroscopy of acetic acid monomer and dimers isolated in solid argon, J. Raman Spectrosc. 42 (2011) 1670–1681.

[15] S. Lopes, A.V. Domanskaya, M. Räsänen, L. Khriachtchev, R. Fausto, Acetic acid dimers in a nitrogen matrix: observation of structures containing the higher-energy conformer, J. Chem. Phys. 143 (2016) 104307.

[16] P.I. Nagy, D.A. Smith, G. Alagona, C. Ghio, Ab initio studies of free and monohydrated carboxylic acids in the gas phase, J. Phys. Chem. 98 (1994) 486–493.

[17] S.F. Boys, F. Bernardi, The calculation of small molecular interactions by the differences of separate total energies. Some procedures with reduced errors, Mol. Phys. 19 (1970) 553–566.

[18] A.L. Picone, C.O. Della Védova, H. Willner, A.J. Downs, R.M. Romano, Experimental and theoretical characterization of molecular complexes formed between OCS and XY molecules (X, Y = F, Cl and Br) and their role in photochemical matrix reactions, Phys. Chem. Chem. Phys. 12 (2010) 563–571.

[19] A.E. Reed, L.A. Curtiss, F. Weinhold, Intermolecular interactions from a natural bond orbital, donor-acceptor viewpoint, Chem. Rev. 88 (1988) 899–926.

[20] W.A. Seth-Paul, Classical and modern procedures for calculating PR separations of symmetrical and asymmetrical top molecules, J. Mol. Struct. 3 (1969) 403–417.

[21] A.P. Scott, L. Radom, Harmonic Vibrational Frequencies: an evaluation of Hartree–Fock, Møller–Plesset, quadratic configuration interaction, density functional theory, and semiempirical scale factors, J. Phys. Chem. 100 (1996) 16502–16513.

[22] R.M. Romano, C.O. Della Védova, A.J. Downs, H. Oberhammer, S. Parsons, Structure and conformational properties of diacetyl sulfide in the gaseous and condensed phases explored by gas electron diffraction, single-crystal X-ray diffraction, vibrational spectroscopy, and quantum chemical calculations, J. Am. Chem. Soc. 123 (2001) 12623–12631.